

LABORATORY LOADING TEST OF TUNNEL SUPPORT WITH YIELDING ELEMENTS IN ISOTROPIC STRESS FIELD

Yota Togashi¹, Takumi Umetsu², Kentaro Nakai³, Fumitaka Mizuno⁴, Kazuo Sakai⁵

Abstract: Yielding elements which have a trilinear stress-strain relationship are often used to prevent support deformation in the mountain tunnel construction for a squeezing rock. Yielding elements are usually placed between shotcrete, and it is expected to have the effect of releasing the radial deformation to the circumferential orientation while maintaining the axial force of the support. Although uniaxial compression tests have been conducted on several types of yielding elements and the evaluation of displacement at actual construction sites where this technology is applied, there are few examples of experimental verification of the mechanical behavior of tunnel support with yielding elements. In this study, tunnel support loading tests on a 1/20 scale were conducted to study the mechanical properties of the tunnel model including yield elements. This experiment can be loaded with nine jacks to the tunnel support model with displacement control. The model was prepared using young aged mortar and ordinary use EPS with a foam ratio of 30 times as yielding elements. Note that rock bolts were not modeled here. The yielding elements were placed on each side wall of the support model, and isotropic compressive loads were gradually applied, assuming a squeezing rock. The results demonstrated that the deformation of the yielding elements to circumferential orientation is dominant as a result of loading. It was also confirmed that the axial force of the tunnel support increases and failure occurs at the point when the yielding elements are almost fully compressed (strain level: 80%). Peak loads leading to failure were almost the same for the cases with and without the yielding elements. The effect of the yielding elements in an isotropic stress field was confirmed in the tunnel support model experiment.

Keywords: Tunnel support loading test, yielding element, squeezing rock, mountain tunnel, shotcrete

1. INTRODUCTION

Yielding elements which have a trilinear stress-strain relationship are often used to prevent tunnel support deformation in the mountain tunnel construction for a squeezing rock [1]. Yielding elements are usually placed between shotcrete, and it is expected to have the effect of releasing the radial deformation to the circumferential orientation while maintaining the axial force of the support. The original idea was to install hard wooden members between concrete linings in the early 1900s [2]. Various types of yielding elements have been developed. For example, hollow or mortar-filled steel pipes are arranged around the circumference of the support [3, 4], hollow steel pipes are laminated to form a honeycomb structure [5], and rectangular concrete mixed with steel fiber or glass beads [6, 7] have been used. In recent years, lightweight yielding element have also been proposed for ease of installation [8]. However, although uniaxial compression tests have been conducted on yielding elements [7, 8]

¹ Ph.D., Togashi, Yota, PE.Jp in construction., Associate Professor, Graduate School of Science and Engineering, Saitama University, 255 Shimo-Okubo Sakura Saitama, Japan, togashi@mail.saitama-u.ac.jp.

² Student, Umetsu Takumi, B. Eng. in Civil Engineering, Graduate School of Science and Engineering Saitama University, 255 Shimo-Okubo Sakura Saitama, Japan, t.umetsu.228@ms.saitama-u.ac.jp.

³ Student, Nakai Kentaro, B. Eng. in Civil Engineering, Graduate School of Science and Engineering Saitama University, 255 Shimo-Okubo Sakura Saitama, Japan, nakai.k.512@ms.saitama-u.ac.jp.

⁴ Research Engineer, Mizuno Fumitaka, M. Sc., Taisei Advanced Center of Technology, Taisei Corporation, 344-1 Nase-cho Totsuka, Yokohama, mznhmt00@pub.taisei.co.jp.

⁵ Senior Research Engineer, Sakai Kazuo, Dr. Eng., Taisei Advanced Center of Technology, Taisei Corporation, 344-1 Nase-cho Totsuka, Yokohama, skikzo01@pub.taisei.co.jp.

and the evaluation of displacement at actual construction sites where this technology is applied [9], there are few examples of experimental verification of the deformation behavior of tunnel support with yielding elements.

On the other hand, in the Japanese railroad industry, tunnel support loading experiments have been conducted since the early 1990s to elucidate the mechanism of tunnel deformation and to confirm the effectiveness of countermeasures [10]. Since the 2000s, large tunnel lining loading test equipment has been developed, and tests have been widely conducted not only in mountain tunnels [11] but also in shielded tunnels [12]. However, we have yet to find a case in which yielding support experiments have been conducted.

In this study, tunnel support loading tests on a 1/20 scale were conducted to study the mechanical properties of the tunnel support model including yield elements. The model was prepared using young aged mortar, assuming shotcrete, and styrene foam of normal use, assuming yielding element. In following chapter, we show the results of loading under isotropic stress assuming a squeezing ground.

2. TUNNEL SUPPORT LOADING TEST

In this study, a tunnel support loading test apparatus was developed as shown in Fig. 1. This device is capable of independently loading a 1/20 sized tunnel support model with nine jacks. Loads can be applied to the tunnel model by applying forced displacement to the rigid loading platen with a screw jack. The depth of the loading plates is 110 mm, and each plate can load the model uniformly in the depth direction. Teflon sheets are placed at the boundary between the loading plate and the support model, and the sheets are also placed at the bottom of the model to follow the large radial displacement due to yielding element deformations. A load cell (Sensor and Control Company Limited. SC301A) is installed directly above the loading platen, and the load can be displayed on a digital monitor (Gravity DFR0009) via a Single Board Computer (Arduino Uno) and amplifier (HX711).

Here, the tunnel model is subjected to a gradually increasing isotropic loading that assumes a squeezing rock. The measurement interval was every 0.05 – 0.1 kN. The loading proceeded by controlling the load so that all load cells had the same value while adjusting 9 screw jacks. Loads were measured with nine load cells, and strain gauges were placed at five locations on the inner edge of the yielding support model (red locations in the figure) to measure the circumferential strain of the tunnel. Displacements of the yielding element model were measured at the radial center during each loading phase. It should be noted that this experiment did not use rock bolts assuming that their effect to be only suspending or sewing support to the ground.

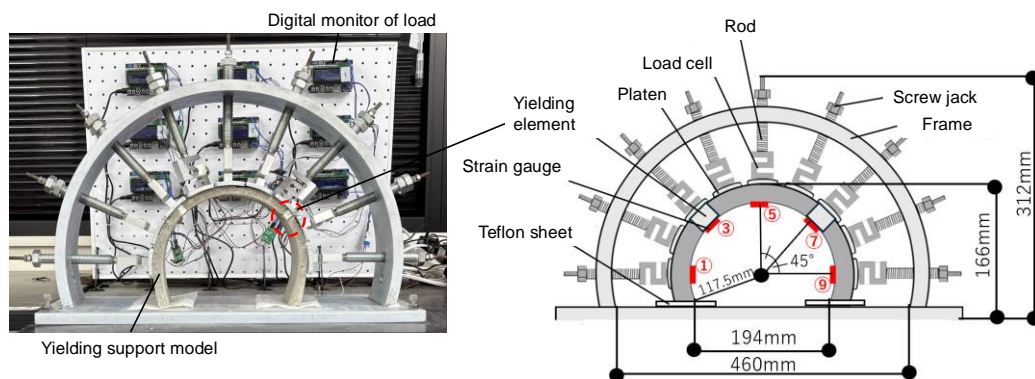


Figure 1. Tunnel support loading test apparatus.

3. MATERIAL PROPERTIES FOR YIELDING SUPPORT MODEL

Figure 2 shows the preparation of the yielding support model in this study. The yielding support model is composed of styrofoam for normal use (30 times the foam ratio, density: 0.0368 Mg / m^3) and a young aged (2-day curing) mortar that assumes shotcrete. The styrene foam has been subjected to uniaxial compression tests, as shown in Fig.3 (a). The dimensions of the uniaxial compression specimen are 40 mm wide, 40 mm deep, and 20 mm high. Fig. 3(b) shows the stress-strain relationship. As can be seen, the trilinear stress-strain relationship was confirmed. As shown in Fig. 3(c), there is almost no lateral displacement and almost no Poisson effect. The mortar was made of 40% ordinary Portland cement, 40% silica sand # 4 (dominant grain size: 0.6 mm - 0.85 mm), and 20% deionized water by weight. The mortar was subjected to uniaxial compression and Brazilian tests, and the mechanical properties are shown in Table 1. The authors proposed a method for estimating Mohr-Coulomb failure

criteria by uniaxial compression and Brazilian tests [13], and this method was used to identify the shear resistance angle ϕ and cohesion c of the mortar. This method has been confirmed to be valid for low stress fields [14].

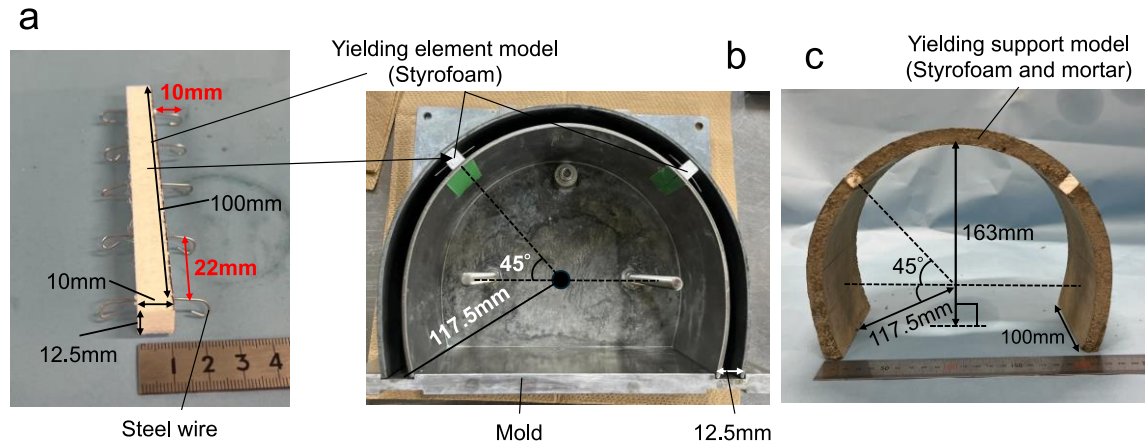


Figure 2. Yielding support model: (a) yielding element model by styrofoam, (b) yield element model setting in the mold, (c) appearance of the model.

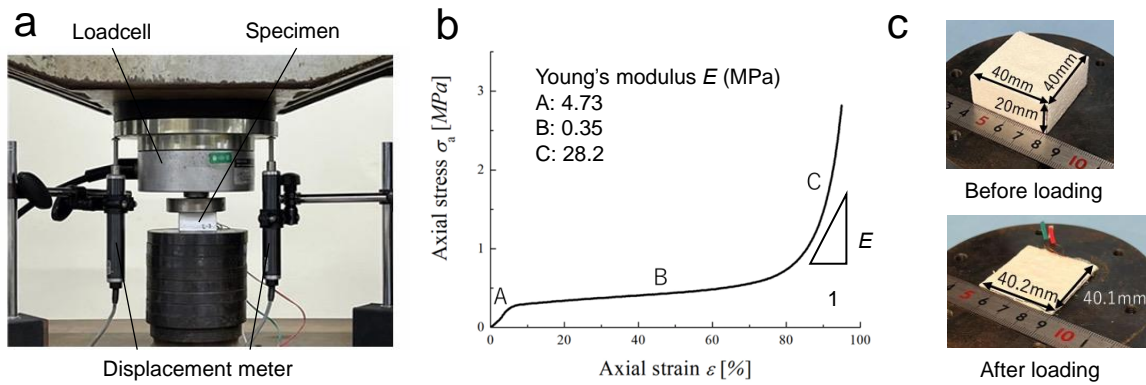


Figure 3. Uniaxial compression test of yielding element: (a) test setting, (b) stress-strain relationship, (c) specimen size and deformation.

Table 1. Mechanical properties of young aged mortar (2-day curing)

Young's Modulus E (MPa)	Uniaxial compressive strength q_u (MPa)	Tensile strength σ_t (MPa)	Shear resistance angle ϕ ($^\circ$)	Cohesion c (MPa)
2333	6.0	0.6	48.8	1.1

Next, the yielding support model is described. As shown in Fig. 2 (a), the yielding element model has a tunnel circumferential length of 10 mm and a radial length of 12.5 mm, the same as the mortar. Steel wires with a hooked end are passed through the yielding element to be fixed after mortar solidification between crown and side wall parts of mortar supports. Two yielding element models are placed symmetrically on the formwork as shown in Fig. 2 (b), and mortar is poured between them. The yielding element was placed on the side of support at 0, 22.5, and 45 degrees inclined from the spring line. After two days of mortar curing, the yielding support model shown in Fig. 2(c) is completed. Note that the inner and outer edges of the mold can be removed separately.

Figure 4 shows test cases studied here. Fig. 4 (a) shows the normal case, a young aged mortar-only specimen. Fig. 4 (b, c, d) shows the experimental cases of yielding support, where yielding elements are placed symmetrically in two tunnel sections at 0°, 22.5°, and 45° from the spring line (SL), respectively, in order to examine the influence of the position of the yielding element. The nine screw jacks are numbered to distinguish loads and radial displacements. Strain gauges were placed at the red points on the inner edges of the tunnel support specimens to measure the circumferential strain. In the case with the red mark on the yielding element, the strain gage was

placed on the mortar at a slightly displaced position. Strain in the yielding element model was calculated from displacements measured at the radial center of the styrofoam.

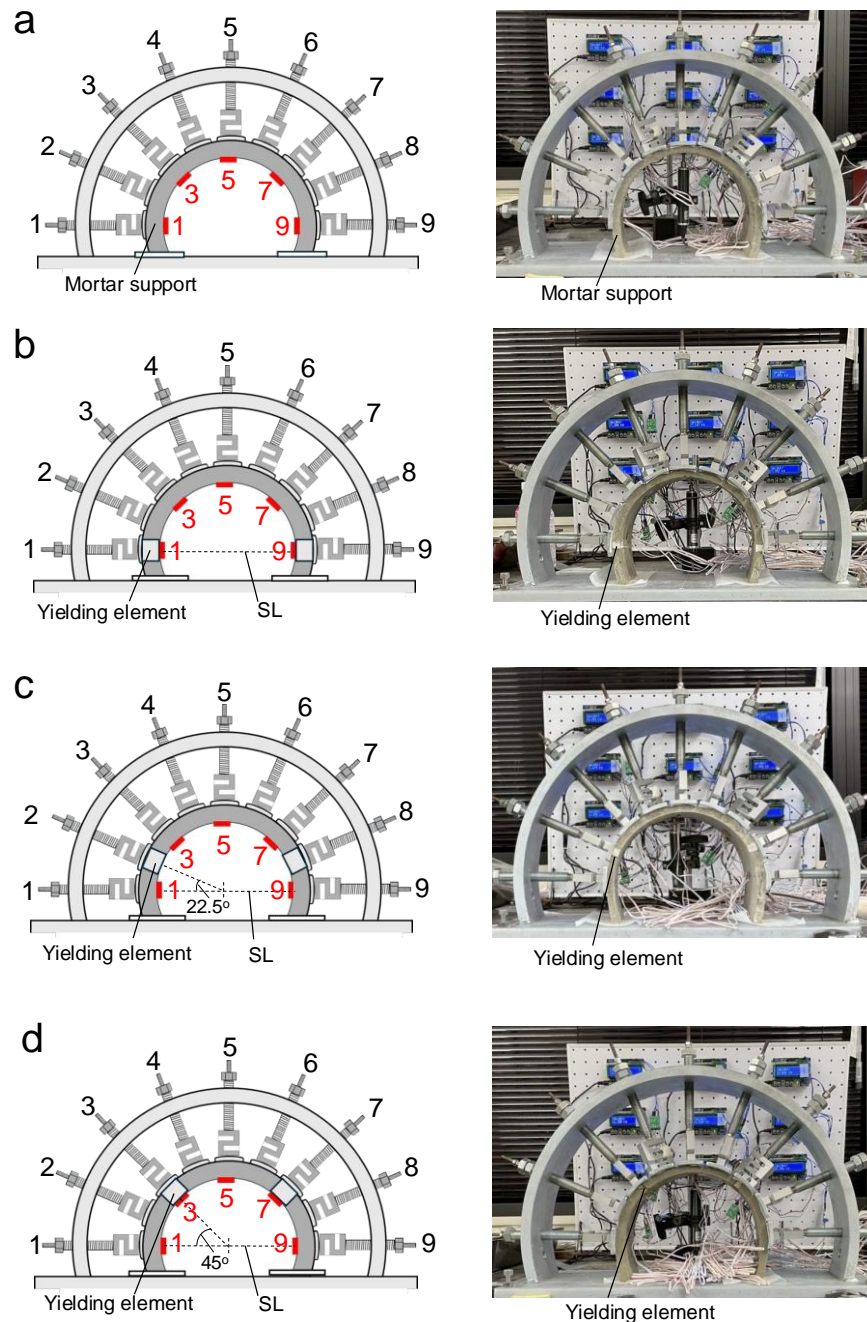


Figure 4. Test cases of tunnel support loading test: (a) normal case (only mortar), (b) case of yielding element on spring line, (c, d) cases with yielding elements at 22.5° and 45° from spring line.

4. TUNNEL SUPPORT LOADING TEST RESULTS

Figure 5 shows the relationship between loading step and isotropic load (loading path) separately for each experimental case. At first, measurements were taken every 0.05 kN or 0.1 kN, and the measurement interval was changed to every 0.2 kN when the loading progressed to a certain degree or when the deformation of the yield element had converged, thus changing the slope of the loading path. The last loading step in this figure represents the load at the end state. Comparing the normal case (a) and the yielding support cases (b,c,d), the ultimate loads are approximately the same or at least 20% smaller in the yielding support case.

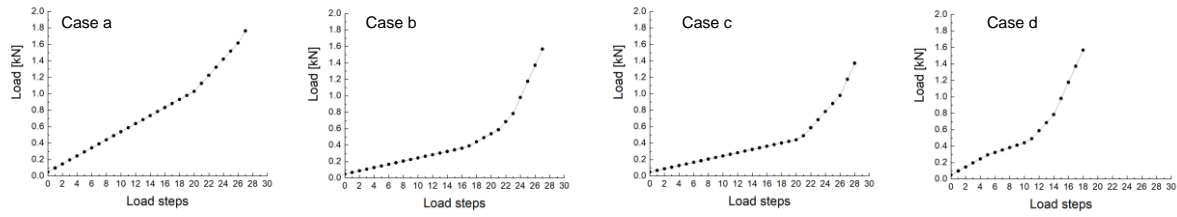


Figure 5. Loading paths for isotropic stress field

Figure 6 (a) shows the relationship between the loading step and the axial displacement of the tunnel crown. In the legend, (A) is the value measured by a contact-type displacement meter, (B) is the value calculated from a screw jack, and (C) is the displacement measured with a ruler for confirmation. Compared to case a without yielding element, the final displacement is about 6.5 times larger in the cases with yielding element. In the yielding support cases (b, c, d), the displacement increases rapidly. As shown later, the deformation of the yielding element increases rapidly at this point (load steps 16 for cases (b, c) and 6 for case (d)). The isotropic load at the point of rapid increase in displacement is about 0.4 kN. Fig. 6 (b) shows the relationship between the displacements of the nine screw jacks and the loading steps. Thus, this figure shows the trend of radial displacement at nine jacking positions. The numbers in the precedents represent the position of the jack in Fig. 4. The displacement is larger in the yielding support case than in the no- countermeasure case (a), and the displacement increases at the points where the yielding support displacement is larger in cases with yielding elements. The characteristic feature here is that the radial displacement above the yielding element is large, and the displacement is smaller toward the bottom end of the tunnel. This is because in Case b, the yielding element is displaced vertically, while in Cases c and d, the yielding element can be displaced horizontally due to these inclined settings. Figure 6(c) shows the relationship between the strain of the yielding element and the loading step. Strain is shown as a positive value in the compression direction. As the displacement of the retractable members increases rapidly as the loading proceeds, the deformation of the tunnel support also increases, as described so far. The isotropic load that causes rapid displacement of the yielding element is about 0.4 kN. Assuming that the same degree of circumferential axial force is applied, the circumferential cross-sectional area of the yielding element is 0.01 m x 0.1 m, which means that normal stress of 0.4 MPa is applied. This corresponds to the stress in the range where Young's modulus is smallest in the stress-strain relationship shown in Fig. 3(b). Since the results are mechanically interpretable, we believe that reasonable experimental results and trends have been obtained.

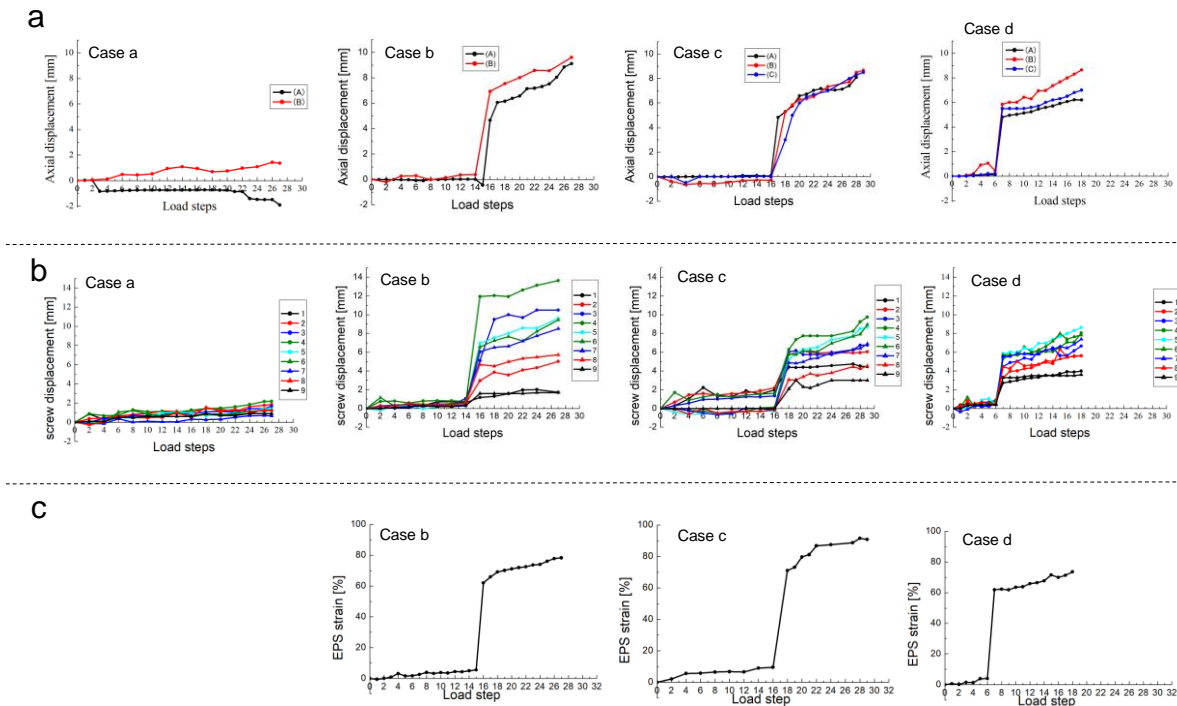


Figure 6. Relationships between load steps, (a) axial, (b) screw jack displacements, and (c) styrene foam strain.

Figure 7 shows the relationship between the loading step and the tunnel circumferential strain measured at several locations on the inner side of the tunnel support. The numbers in the legends correspond to the measurement positions in Fig. 4. These represent strains in the mortar section equivalent to shotcrete, and the differences in the magnitude of the measured values are about the same. Most of the data show values in the compressive direction (positive), which is due to the isotropic loading. On the other hand, there is a large variation, with many data showing strain in the tensile direction (negative). This may be due to the fact that the tunnel shape is not a perfect circle and the inside of the tunnel support is susceptible to bending.

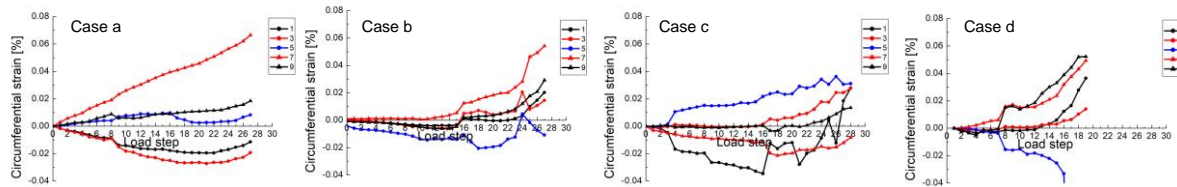


Figure 7. Relationships between load steps and circumferential strain

5. DISCUSSION

In order to further understand the deformation mechanism of yielding support, we first discuss the properties of the specimen at failure. Figure 8 shows some photographs of the specimens after the loading test. In both the three cases with and without yielding elements, the crown of the tunnel support specimen cracked, leading to failure. Similar failure conditions and ultimate loads were observed in the no-countermeasure and yielding support cases. Therefore, it can be said that the yielding element allows radial displacement in squeezing rock and retains some of the strength of the support even after it is fully compressed. In addition, Fig. 8, together with the radial displacement results in Fig. 6 (b), suggests that this is a flexural-tensile failure, since the deformation at the top of the supported specimen is large in all experimental cases, including normal Case a.

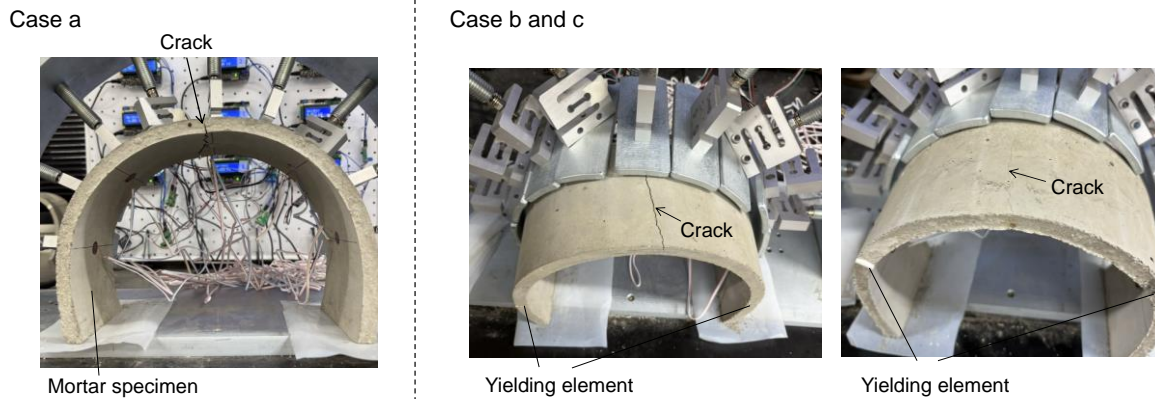


Figure 8. Examples of tunnel support specimen after ultimate load condition

To confirm that the yielding element behaves as expected, Fig. 9 shows the relationship between the isotropic load applied to the specimen in the tunnel support loading experiment and the strain in the yielding element model. Thus, a trilinear relationship is obtained in all cases, and the strain levels at which the slope changes in Fig. 3(b) (A, B, and C in Fig. 3(b)) are approximately equal. According to the calculation at the load level where the deformation increases as discussed in Fig. 6, the tunnel circumferential axial force equivalent to the applied isotropic load acts on the yielding element. Since the same deformation behavior of the yielding element is obtained in the three experimental cases of yielding support, the position of the yielding element does not affect the deformation in an isotropic stress field.

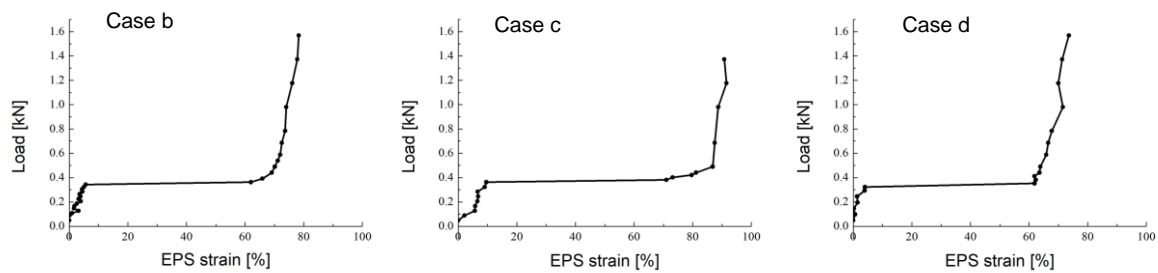


Figure 9. Relationship between isotropic load and yielding element strain in tunnel support loading tests

6. CONCLUSIONS

In this study, tunnel support loading experiments were conducted to experimentally understand the mechanical behavior of tunnel supports including yielding elements. As a result, the following findings were obtained.

- In this study, we employed a tunnel support model with two symmetrically installed yield elements, and conducted experiments with three different positions of the yielding element.
- At strain levels where the displacement of the yielding element increases rapidly, the deformation of the yielding support increases rapidly.
- The yielding support fails after the yielding element has been fully compressed, at a load equivalent to that of a shotcrete equivalent mortar specimen.
- When the yielding element is placed at an angle, the deformation of the yielding element causes horizontal displacement. On the other hand, if the yielding element is placed near vertical, only vertical displacement will occur. The deformation of yielding support depends on the position of the yielding element.
- The mechanical behavior of tunnel supports containing yielding elements was clarified experimentally for the first time in laboratory scale.

7. ACKNOWLEDGEMENT

Mr. Oishi K, a fourth-year undergraduate student at the Rock Mechanics Laboratory of Saitama University, assisted in conducting the experiments in this study. We would like to express our gratitude for his cooperation.

8. REFERENCES

- [1] Wittke, W. (2014). Rock Mechanics Based on an Anisotropic Jointed Rock Model (AJRM). Wiley, 91-114.
- [2] Kovári, K. (2009). Design methods with yielding support in squeezing and swelling rocks. Proc. World Tunnel Congress 2009, 1-10.
- [3] Schubert, W. (1996). Dealing with squeezing conditions in alpine tunnels. Rock Mech Rock Eng, 29(3), 145-153.
- [4] Sakai, K., Schubert, W. (2019). Study on ductile support system by means of convergence confinement method. Proceedings of ISRM2019 Specialized Conference, YSRM2019 & REIF2019, 1-6.
- [5] Podjadtke, R. (2009). Development and application of stress controllers – system honeycomb – in modern tunnelling. Proceedings of Shotcrete for Underground Support XI, 1-9.
- [6] Thut, A., Steiner, P., Stolz, M. (2006). Tunnelling in Squeezing Rock-Yielding Elements and Face Control. Proc. 8th International Conference on Tunnel Constructions and Underground Structures, 1-7.
- [7] Ohara, N., Kaneko, T., Sakai, K., Tani, T., Ichida, T. (2017). Study of design methodology and applicability of yielding support for tunnelling. Proc. 45th Rock mechanics symposium, 103-108. (In Japanese)
- [8] Entfellner, M., Hamdi, P., Wang, X., Wannenmacher, H., Amann, F. (2023). Investigating High-Strength Expanded Polystyrene (HS-EPS) as yielding support elements for tunnelling in squeezing ground conditions. Tunnelling and Underground Space Technology, 140, 105261.
- [9] Entfellner, M., Wannenmacher, H., Schubert, W. (2023). Yielding elements made of high-strength expanded polystyrene (HS-EPS). Proc. Expanding Underground. Knowledge and Passion to Make a Positive Impact on the World, 1864-1871.
- [10] Asakura, T., Kojima, Y., Ando, T., Sato, Y., Matsuura, A. (1994). Fundamental study on static deformation behavior of tunnel lining. Proc. JSCE, 493, 79-88. (In Japanese)

- [11] Yashiro, K., Kojima, Y., Arai, Y., Okano, N., Takemura, J. (2009). A study on numerical simulation method for plain concrete tunnel lining considering softening due to compression failure. *Proc. JSCE*, 65(4), 1024-1038. (In Japanese)
- [12] Tsuno, K., Kinoshita, K., Ushida, T. (2020). Investigation of deformation of shield tunnel based on large-scale model test. *QR of RTRI*, 61(1), 16-21.
- [13] Kotabe, H., Togashi, Y., Osada, M., Hatakeyama, K. (2024). Unsaturated strength of tuff and its water retention drying curve. *J Soc Mater Sci Japan*, 73(3), 212-219.
- [14] Togashi, Y., Kotabe, H., Osada, M., Asamoto, S., Hatakeyama, K. (2025). Strength changes associated with water transport in unsaturated tuff during drying. *Int J Rock Mech Min Sci*, 186, 105984.